

LC–MS Metabolomics of Psoriasis Patients Reveals Disease Severity-Dependent Increases in Circulating Amino Acids That Are Ameliorated by Anti-TNF α Treatment

Muhammad Anas Kamleh,^{†,⊥} Stuart G. Snowden,^{†,⊥} Dmitry Grapov,[‡] Gavin J. Blackburn,[§] David G. Watson,[§] Ning Xu,^{||} Mona Ståhle,^{*,||} and Craig E. Wheelock^{*,†}

[†]Department of Medical Biochemistry and Biophysics, Division of Physiological Chemistry 2, Karolinska Institutet, SE-17177 Stockholm, Sweden

[‡]NIH West Coast Metabolomics Center, University of California, Davis, California 95616, United States

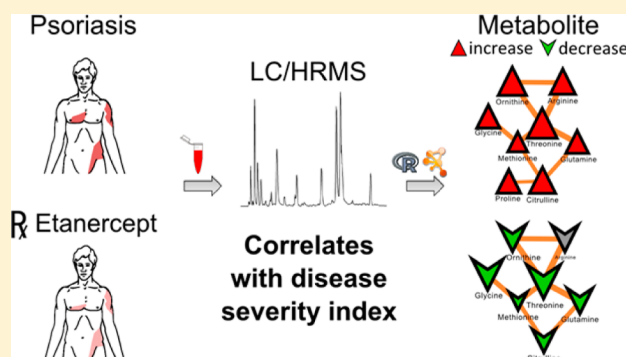
[§]Strathclyde Institute of Pharmacy and Biomedical Science, 161 Cathedral Street, Glasgow G4 0RE, United Kingdom

^{||}Dermatology Unit, Department of Medicine, Karolinska Institutet, SE-17176 Stockholm, Sweden

S Supporting Information

ABSTRACT: Psoriasis is an immune-mediated highly heterogeneous skin disease in which genetic as well as environmental factors play important roles. In spite of the local manifestations of the disease, psoriasis may progress to affect organs deeper than the skin. These effects are documented by epidemiological studies, but they are not yet mechanistically understood. In order to provide insight into the systemic effects of psoriasis, we performed a nontargeted high-resolution LC–MS metabolomics analysis to measure plasma metabolites from individuals with mild or severe psoriasis as well as healthy controls. Additionally, the effects of the anti-TNF α drug Etanercept on metabolic profiles were investigated in patients with severe psoriasis. Our analyses identified significant psoriasis-associated perturbations in three metabolic pathways: (1) arginine and proline, (2) glycine, serine and threonine, and (3) alanine, aspartate, and glutamate. Etanercept treatment reversed the majority of psoriasis-associated trends in circulating metabolites, shifting the metabolic phenotypes of severe psoriasis toward that of healthy controls. Circulating metabolite levels pre- and post-Etanercept treatment correlated with psoriasis area and severity index (PASI) clinical scoring ($R^2 = 0.80$; $p < 0.0001$). Although the responsible mechanism(s) are unclear, these results suggest that psoriasis severity-associated metabolic perturbations may stem from increased demand for collagen synthesis and keratinocyte hyperproliferation or potentially the incidence of cachexia. Data suggest that levels of circulating amino acids are useful for monitoring both the severity of disease as well as therapeutic response to anti-TNF α treatment.

KEYWORDS: Mass spectrometry, metabolomics, psoriasis, pathway enrichment, HILIC, keratinocyte, collagen, Etanercept, diabetes



INTRODUCTION

Psoriasis is an immune-mediated skin disease associated with significant morbidity and mortality.¹ The ultimate cause of psoriasis remains unclear, but it involves triggering the immune system, leading to sustained inflammation and dysregulation of keratinocyte differentiation.² Psoriasis is a heterogeneous disease with significant comorbidities including, in particular, psoriatic arthritis.^{3–5} Genome-wide association studies indicate a large genetic component in the pathogenesis of psoriasis.⁶ In particular, the HLA-C gene is estimated to contribute ~50% to the heritability in early onset psoriasis.⁷ Once activated, dendritic cells stimulate differentiation and migration of Th1 and Th17 effector T cells to the skin, which, through cytokine release, immune cell recruitment, and keratinocyte proliferation, drive a sustained cycle of chronic inflammation.⁸ Patients

with psoriasis are also at a significant risk of developing metabolic syndrome, type 2 diabetes, hypertension, and obesity.^{9–11} The underlying mechanisms are still unclear, and, to date, comorbidities are supported primarily by epidemiological data.¹²

The cytokine tumor necrosis factor alpha (TNF α) is known to play a major role in the pathophysiology of psoriasis,¹³ and anti-TNF α therapeutics are routinely used to treat immune-mediated diseases including psoriasis as well as psoriatic and rheumatoid arthritis in adult as well as pediatric populations.^{5,14} One of the first-line anti-TNF α treatments is the biologic

Special Issue: Environmental Impact on Health

Received: August 2, 2014

Published: October 31, 2014

Etanercept, which has demonstrated efficacy in resolving psoriatic lesions. Etanercept is a fusion protein that binds to the constant end of the IgG1 antibody^{5,15} and acts as a competitive inhibitor of TNF α . Although it significantly suppresses the associated inflammation, Etanercept, as well as other biologic therapeutics, does not cure the underlying disease.¹⁶ TNF α is also involved in other physiological processes such as muscle protein proteolysis and cachexia,¹⁷ thereby suggesting additional pathways by which anti-TNF α therapeutics may affect the underlying pathophysiology of the disease.

In order to investigate the systemic biochemical shifts associated with disease severity, liquid chromatography high-resolution mass spectrometry (LC–HRMS) metabolomic analysis was used to characterize circulating metabolites in psoriasis patients. Metabolomics profiles were also compared before and after a 12 week treatment with Etanercept. A metabolomics-based research approach involves simultaneously analyzing the complement of small molecules (metabolites) in a system. This has been shown to be useful for identifying metabolic traits that represent intermediate phenotypes capable of linking genetic and environmental factors to heterogeneous diseases.^{18,19} This study is, to the best of our knowledge, the first to examine the metabolic profile associated with plaque psoriasis severity and the effects of Etanercept treatment. These results provide insight into the biochemical pathways involved in the etiology of psoriasis and the systemic effects of Etanercept treatment.

■ EXPERIMENTAL SECTION

Study Design

Healthy controls as well as patients with mild or severe psoriasis were recruited at the Karolinska University Hospital. Mild psoriasis patients were recruited from a cohort of patients with newly onset psoriasis who did not require systemic therapy and were therefore treated only topically. Severe psoriasis patients required systemic therapy to control the skin manifestations of the disease. None of the patients were on statins or prescribed anti-inflammatory drugs. All samples were obtained prior to the commencement of any treatment. The recruitment group consisted of 96 gender-balanced individuals (32 healthy controls and 32 mild and 32 severe psoriasis). For analysis purposes, the full cohort ($n = 96$) was subdivided into two gender- and disease severity-balanced groups ($n = 48$ each), called exploratory and validation cohorts (Table 1). The exploratory cohort was used to identify metabolic markers for psoriasis severity, and the validation cohort as a confirmation of the identified trends. Additional plasma samples were taken from the severe psoriasis patients ($n = 16$) in the validation cohort following 12 weeks of Etanercept (Enbrel) treatment (50 mg once per week subcutaneously), and this group is referred to as the treatment cohort. For blood collection, 10 mL of whole blood was collected in EDTA tubes after overnight fasting. Samples were left standing for 1 h before centrifugation at room temperature for 20 min at 3100 rpm. After centrifugation, samples were aliquoted and immediately stored at -70°C until use. Psoriasis disease was judged as severe when it required systemic therapy and was evaluated by the psoriasis area and severity index (PASI), which is an established measurement that quantifies the thickness, redness, scaling, and distribution of psoriasis lesions.²⁰ The study was approved by the Regional Committee of Ethics and was performed

according to the Declaration of Helsinki Principles. Signed consent forms were collected from all sample donors.

HILIC Mode Metabolomics

A cocktail of four internal standards (10 μL ; Table S1) was added to 50 μL of EDTA plasma. Proteins were precipitated using 200 μL of HPLC grade acetonitrile (Rathburn). Samples were vortexed for 5 s and then left to stand on ice for 10 min followed by centrifugation at 15 000 rcf for 10 min at 4°C . The supernatant (150 μL) was transferred to a clean Eppendorf tube, and 20 μL of each sample was used to produce a pooled quality control. Samples were stored at -20°C prior to analysis. Prepared samples were analyzed on a Thermo Ultimate 3000 HPLC and Thermo Q-Exactive (Orbitrap) mass spectrometer. Ten microliters of sample was injected on a Merck Sequant ZIC-HILIC column (150 \times 4.6 mm, 5 μm particle size) coupled to a Merck Sequant ZIC-HILIC guard column (20 \times 2.1 mm). Mass spectrometry data were acquired (full scan mode) in both positive and negative ionization modes, using 140 000 mass resolution.

Reversed-Phase (RP) Metabolomics

A cocktail of five internal standards (10 μL ; Table S1) was added to 50 μL of EDTA plasma followed by 150 μL of chilled (-20°C) methanol (Rathburn) for protein precipitation. Samples were vortexed for 5 s and left to stand for 2 h at -20°C , followed by centrifugation at 15 000 rcf for 12 min at 4°C . The supernatant (90 μL) was transferred to a clean Eppendorf tube, and 10 μL of each sample was used to produce a pooled quality control. On the analysis day, samples were diluted 1:1 with Milli-Q water (Millipore). Prepared samples were analyzed on a Thermo Ultimate 3000 HPLC and Thermo Q-Exactive (Orbitrap) mass spectrometer. Twenty microliters of sample was injected on a Thermo Accucore aQ RP C18 column (150 \times 2.1 mm, 2.7 μm particle size). Mass spectrometry data were acquired (full scan mode) in both positive and negative ionization modes, using 70 000 mass resolution. Detailed methods are provided in the Supporting Information.

Data Processing and Metabolite Annotation

RAW files were converted to universal mzXML file using MSconvert.²¹ All chromatograms were evaluated using the open source software package XCMS²² performed in R.²³ For the preliminary analysis, metabolites were annotated by matching accurate mass and retention time (AMRT) to authentic chemical reference standards. Variables of importance identified from the multivariate analyses (see Statistical Analysis) were subjected to further identity confirmation by comparing fragmentation patterns to those of chemical standards. The MS/MS spectra of all reported metabolites matched those of the standards with the exception of inosine (which was excluded from further analysis). Data analysis was limited to metabolites matching the AMRT and MS/MS fragmentation spectra of standards except for sphingosine-1-phosphate and GlcCer(C16:0), which were identified only by AMRT. The coefficient of variance (CV) of the HILIC internal standard cocktail was <35%, and for reversed-phase, <15%. All CVs of the discussed metabolites were <30%, except for cystathionine and cytidine (exploratory and validation cohorts) and cysteine and proline (validation cohort only). The median CV for the identified metabolites was 14.8 and 16.0% for the exploratory and validation cohorts, respectively.

Statistical Analysis

Statistical analysis was used to identify significantly altered metabolites within the exploratory and validation cohorts between (1) control and mild, (2) control and severe, (3) mild and severe, and (4) severe pre- and post-treatment with Etanercept (validation cohort only) psoriasis patients. Comparisons for 1–3 were made using two-sample *t*-tests, and for 4, based on a paired *t*-test carried out in the R statistical programming environment.²³ The false discovery rate (FDR) due to the multiple hypotheses tested was adjusted according to Benjamini and Hochberg ($q = 0.05$)²⁴ and reported as p_{adj} . FDR was also directly estimated according to Dabney and Storey²⁵ and reported as the *q*-value.

Multivariate analysis was performed using a combination of principal component analysis (PCA) and orthogonal projection to latent structures–discriminant analysis (OPLS-DA) using SIMCA-P 13 (Umetrics, Umeå, Sweden). OPLS-DA was conducted following logarithmic transformation (base 10), mean centering, and scaling to unit variance (UV). OPLS-DA model performance was evaluated based on the cumulative coefficient of correlation between group labels (*Y*) and model projection of metabolites (*X*) (R^2Y_{cum}) and 7-fold cross-validated model fit to the data (Q^2_{cum}), the significance of which was assessed through cross-validation analysis of variance (CV-ANOVA). Model predictive and orthogonal components are reported as (predictive + orthogonal). Iterative feature selection (2 rounds) was performed to identify important metabolic discriminants between the compared populations. Metabolites were retained in the model based on a combination of variable importance in projection (VIP) > 1.0 and absolute magnitude of correlation with model scores ($p_{\text{corr}} > 0.4$).²⁶ SIMCA-P was used to calculate the PLS inner relation between disease severity score (PASI) and correlated metabolites (|Pearson's correlations| > 0.5).

Pathway Enrichment Analysis

Biochemical pathway enrichment analysis was used to identify psoriasis-dependent changes in global biochemical domains. MetaboAnalyst²⁷ was used to test for significant enrichment in KEGG pathways (<http://www.genome.jp/kegg/>) among the noted metabolic perturbations in common to both the exploratory and validation cohorts (Table 2). Significant enrichment was assessed on the basis of the false discovery rate-adjusted hypergeometric test statistic ($p \leq 0.05$), and impact on pathway topology was defined based on relative-betweenness centrality.

Partial Correlation Network Analysis

Gaussian graphical model networks were calculated for metabolite relationships in the context of the identified differences between (1) control and severe, (2) control and treated severe, and (3) untreated and treated severe psoriasis patients from the validation cohort. *q*-order partial correlations ($q = 1, 12, 24, 35$)²⁸ were calculated ($n = 1000$) in R (v3.0.1)²³ between metabolites ($n = 93$) from the validation data set, excluding patients with mild psoriasis ($n = 48$). To maximize network node inclusion and minimize edge degree, a threshold of $\beta = 0.4$ for the average nonrejection rate (β) for metabolite pairwise relationships was selected. Using this approach, a smaller average nonrejection rate corresponds to stronger *q*-order partial correlation. Spearman's rank order coefficients of correlation, *p*-values, and FDR-adjusted *p*-values (p_{adj})²⁴ were calculated for all *q*-order selected relationships. Cytoscape²⁹ was used to generate network visualizations for all edges

displaying $p_{\text{adj}} \leq 0.05$ (83 edges or 90% of the original *q*-order calculated edges). Network mapping was used to encode and display statistical and multivariate analysis results within the context of the partial correlation defined relationships.

RESULTS

Psoriasis patients and control characteristics were consistent between the exploratory and validation cohorts (Table 1). PASI

Table 1. Characteristics of the Study Cohorts^a

	exploratory cohort		
	control	mild	severe
gender	8/8 ^d	8/8	8/8
age (years)	52 ± 9	52 ± 8	58 ± 10
BMI ^b	26.1 ± 4.1	25.0 ± 4.8	28.4 ± 3.5
PASI ^c	n/a	1.4 ± 0.7 ^e	16.5 ± 7.4 ^e
cholesterol	5.2 ± 0.8	5.1 ± 0.9	4.8 ± 0.9
triglycerides	1.0 ± 0.4	1.0 ± 0.56	1.3 ± 0.5

	validation cohort			
	control	mild	severe	severe (treated) ^f
gender	8/8	8/8	8/8	8/8
age (years)	44 ± 13	42 ± 20	53 ± 13	53 ± 13
BMI	24.0 ± 3.1	25.2 ± 4.7	27.3 ± 4.8	27.2 ± 4.6
waistline (cm)	n/d	n/d	98 ± 13.8	97 ± 12.9
PASI	n/a	1.6 ± 1.0 ^e	13.6 ± 4.5 ^e	4.9 ± 3.4 ^g
cholesterol	5.1 ± 0.8	4.9 ± 0.9	5.3 ± 0.6	6.57 ± 4.1 ^h
triglycerides	1.1 ± 0.6	1.2 ± 1.0	1.0 ± 0.4	1.7 ± 0.9

^aValues are reported as the mean ± SD. Units for cholesterol and triglycerides are mmol/L. n/d indicates that the value was not determined. ^bBMI, body mass index. ^cPASI, psoriasis area and severity index. There is no PASI score for the control group (n/a). ^dGender balance: male/female. ^e*p*-value < 0.05 for a two-sample *t*-test for the PASI score between mild and severe psoriasis subjects. ^fSevere psoriasis patients treated with Etanercept for 12 weeks. ^g*p*-value < 0.05 for a paired two-sample *t*-test for the PASI score for treated vs untreated severe psoriasis. ^h*p*-value < 0.05 based on a paired *t*-test.

scoring significantly increased ($p < 0.05$) with disease severity in both cohorts and decreased following Etanercept treatment (Table 1). HILIC mode and reversed-phase metabolomic analyses of the exploratory and validation cohorts' plasma were used to identify 94 and 93 metabolites from the XCMS diffeport of all samples, respectively (67 of which were in common), through matching of retention time and spectra to external standards (Table S2). Statistical analyses of the metabolomic measurements with adjustment for FDR were used to identify significantly altered compounds among control, mild, and severe psoriasis patients for both the exploratory and validation cohorts (Tables S3 and S4) and between severe and severe Etanercept-treated psoriasis patients in the validation cohort (Table S4). Additionally, changes in >150 metabolite features putatively identified based on only accurate mass are reported for the comparisons between severe psoriasis patients and controls in both cohorts (Tables S5 and S6) and between severe psoriasis patients at baseline and after Etanercept treatment (Table S7).

As expected, the largest effect size was observed between control and severe psoriasis patients, with 33 and 34 significantly ($p_{\text{adj}} \leq 0.05$) perturbed plasma metabolites in the exploratory and validation cohorts, respectively (Tables S3 and S4). Comparison of the psoriasis-associated metabolic alter-

Table 2. Fold Changes in Metabolites Associated with Severe Psoriasis That Showed Similar Patterns in the Exploratory and Validation Cohorts

pathway	metabolite ^a	exploratory cohort		validation cohort		Etanercept treated cohort			
		severe vs control ^b		severe vs control		treated vs severe		treated vs control	
		q-value ^c	FC ^d	q-value	FC	q-value	FC	q-value	FC
arginine and proline pathway ^e	arginine ^o	1.82×10^{-2}	2.47	1.43×10^{-3}	2.29	7.58×10^{-3}	0.45	7.48×10^{-1}	1.02
	citrulline ^o	4.09×10^{-4}	2.61	1.16×10^{-5}	1.88	1.46×10^{-2}	0.64	4.07×10^{-1}	1.19
	ornithine ^o	6.92×10^{-3}	3.37	1.77×10^{-4}	2.92	2.18×10^{-3}	0.41	4.07×10^{-1}	1.21
	proline ^o	1.24×10^{-2}	1.83	1.40×10^{-2}	1.89	1.09×10^{-1}	0.65	4.16×10^{-1}	1.22
	hydroxyproline ^o	2.16×10^{-2}	2.93	6.88×10^{-3}	1.81	7.87×10^{-2}	0.69	3.99×10^{-1}	1.25
glycine, serine, and threonine pathway ^f	glycine ^o	9.42×10^{-3}	2.13	2.87×10^{-3}	1.68	2.18×10^{-3}	0.49	3.99×10^{-1}	0.83
	serine ^o	4.74×10^{-3}	1.96	1.15×10^{-4}	1.61	1.35×10^{-1}	0.78	3.58×10^{-1}	1.25
	threonine ^o	4.09×10^{-4}	2.68	3.99×10^{-6}	2.58	7.77×10^{-7}	0.32	3.85×10^{-1}	0.82
alanine, aspartate, and glutamate pathway ^g	aspartate ^o	7.66×10^{-3}	2.43	2.63×10^{-5}	1.96	1.39×10^{-1}	0.69	3.99×10^{-1}	1.34
	glutamate ^o	1.26×10^{-2}	3.00	4.80×10^{-3}	2.22	3.33×10^{-1}	0.78	3.58×10^{-1}	1.72
	glutamine ^o	1.75×10^{-3}	2.03	4.26×10^{-4}	1.71	7.34×10^{-3}	0.59	7.48×10^{-1}	1.02
cysteine and methionine pathway ^h	cystine ^o	4.07×10^{-3}	2.81	1.77×10^{-4}	1.83	2.86×10^{-1}	0.9	6.07×10^{-3}	1.64
	cystathionine ^o	1.13×10^{-2}	0.83	3.99×10^{-6}	0.31	2.96×10^{-1}	1.51	1.94×10^{-2}	0.47
	methionine ^o	1.41×10^{-2}	2.15	1.77×10^{-4}	1.84	4.82×10^{-5}	0.42	3.58×10^{-1}	0.78
taurine and hypotaurine pathway ⁱ	taurine ^o	2.70×10^{-4}	1.92	4.96×10^{-4}	1.47	1.79×10^{-1}	0.82	3.38×10^{-1}	1.21
phenylalanine pathway ^j	phenylalanine ^o	1.90×10^{-2}	1.34	1.89×10^{-4}	1.48	4.52×10^{-2}	0.73	5.38×10^{-1}	1.07
pyrimidine pathway ^k	cytidine ^o	7.80×10^{-3}	2.09	2.55×10^{-2}	2.47	2.42×10^{-1}	0.65	3.58×10^{-1}	1.6
amino sugar pathway ^l	acetylglucosamine ^o	6.92×10^{-3}	2.36	2.90×10^{-3}	1.34	7.87×10^{-2}	0.72	7.12×10^{-1}	0.96
sphingolipid pathway ^m	glucosylceramide (C16:0) ^p	4.29×10^{-2}	1.46	1.01×10^{-2}	1.59	4.34×10^{-1}	0.95	3.02×10^{-1}	1.51
	sphingosine-1-phosphate ^p	3.54×10^{-2}	1.21	1.89×10^{-4}	1.93	3.06×10^{-1}	0.88	2.94×10^{-2}	1.69

^aAll metabolites displayed were not significantly altered in mild vs control or mild vs severe psoriasis patients in either the exploratory or validation cohorts. ^bSevere psoriasis patients vs healthy controls. ^cFalse discovery rate (FDR) was directly estimated according to the methods of Dabney and Storey.²⁵ ^dFold change between the two groups. ^eKEGG Pathway map hsa00330: arginine and proline metabolism. ^fKEGG Pathway map hsa00260: glycine, serine, and threonine metabolism. ^gKEGG Pathway map hsa00250: alanine, aspartate, and glutamate metabolism. ^hKEGG Pathway map hsa00270: cysteine and methionine metabolism. ⁱKEGG Pathway map hsa00430: taurine and hypotaurine metabolism. ^jKEGG Pathway map hsa00360: phenylalanine metabolism. ^kKEGG Pathway map hsa00240: pyrimidine metabolism. ^lKEGG Pathway map hsa00520: amino sugar and nucleotide sugar metabolism. ^mKEGG Pathway map hsa00600: sphingolipid metabolism. ^oResults obtained from HILIC analysis. ^pResults obtained from reversed-phase analysis.

ations in common to both cohorts identified 20 significantly ($p_{\text{adj}} \leq 0.05$) altered metabolites, 17 of which increased with psoriasis severity in both cohorts (Table 2). In particular, ornithine and another urea cycle intermediate, citrulline, increased by 215 and 90%, on average, respectively, in severe psoriasis patients compared to that in controls (Table 2). Etanercept treatment led to reductions in 10 of the 20 (50%) previously identified psoriasis-associated metabolic dysregulations (Table 2). Specifically, treatment resulted in significant reductions in amino acids, highlighted by 230, 233, and 150% decreases in threonine, ornithine, and methionine, respectively (Table 2). Comparison of Etanercept-treated severe psoriasis to controls revealed a normalization in the majority (89%) of metabolites previously shown to be increased with disease. Although cystine was significantly reduced by 10% following treatment, this amino acid remained 60% elevated in the treated group relative to that in controls (Table 2). Cystathionine was the only metabolite in common to both cohorts that was reduced (80%) in severe psoriasis compared to that in controls and was not significantly affected by Etanercept treatment (Table 2). Similarly, sphingosine-1-phosphate levels were not affected by treatment and remained 70% elevated in the treated group (Table 2).

The relationship between psoriasis disease severity score (PASI) and the metabolites identified in Table 2 was further interrogated using correlation analysis and partial least-squares (PLS) inner relation. Of the metabolites presented in Table 2,

10 correlated with psoriasis disease severity scores ($r \geq 0.5$) in either the validation or treated cohort (Table 3). A PLS inner relation was calculated between these 10 metabolites and PASI scores (Figure 1), producing a significant multivariate association ($R^2 = 0.80$; $p < 0.0001$) between PASI scores (Figure 1A) and metabolite abundances (Figure 1B). Threonine, citrulline, and ornithine displayed the highest positive correlation with PASI scores (Table 3), whereas threonine, glutamine, and ornithine were the most highly ranked multivariate predictors of psoriasis severity (Figure 1B). Following Etanercept treatment, there was a significant reduction in PASI scores associated with a normalization in all but two of the metabolites that were altered in severe psoriasis patients within both cohorts (Table 2).

Data sets were further interrogated using multivariate methods. PCA identified no outliers in the exploratory or validation cohorts based on Hotelling's T^2 (i.e., 95% confidence interval) or DModX (data not shown). Multivariate classification modeling (OPLS-DA) followed by feature selection was implemented to identify top metabolic markers for disease-specific differences in plasma metabolite profiles in both cohorts (Figure 2 and Table S8). For the exploratory cohort, only severe psoriasis produced significant models ($p < 0.05$; mild vs severe [$Q^2 = 0.605$]; control vs severe [$Q^2 = 0.741$]). For the validation cohort, all calculated models were significant ($p < 0.001$) and showed a disease severity-based increase in circulating metabolites from control vs mild ($Q^2 = 0.626$) to

Table 3. Pearson's Correlations between Disease Severity (PASI) and Plasma Metabolite Levels^a

metabolite	exploratory cohort ^b	validation cohort ^b	treated cohort ^{b,c}
arginine	0.52**	0.50***	0.60**
citrulline	0.73***	0.84***	0.70***
ornithine	0.43*	0.84***	0.75***
proline	0.77***	0.23	0.37*
hydroxyproline	0.20	0.43*	0.23
glycine	0.74***	0.47***	0.69***
serine	0.44**	0.73***	0.55**
threonine	0.84***	0.87***	0.88***
aspartate	0.05	0.26	0.17
glutamate	0.33	0.42*	0.09
glutamine	0.70***	0.66***	0.76***
cystine	0.79***	0.75***	0.56**
cystathionine	-0.27	-0.43	-0.19
methionine	0.39*	0.46**	0.74***
taurine	0.34	0.51**	0.22
phenylalanine	0.31	0.66**	0.37*
cytidine	0.63***	0.36*	0.34
acetylglucosamine	0.28	0.48**	0.45*
glucosylceramide (C16:0)	0.50**	0.34	0.19
sphingosine-1-phosphate	0.35	0.50*	0.16

^aMetabolites in the validation and treated cohorts with $r \geq 0.5$ were used for the regression with PASI score in Figure 1. Correlations include both mild and severe psoriasis patients for both the exploratory and validation cohorts. ^bThe significance level is indicated as follows: *, $p < 0.05$; **, $p < 0.01$; ***, $p < 0.001$. The confounding effects of age and BMI were tested via a linear regression model using STATA 11. ^cSevere psoriasis patients from the validation cohort were treated with Etanercept for 12 weeks. Correlation values are only for the treated patients.

mild vs severe ($Q^2 = 0.794$) to control vs severe ($Q^2 = 0.891$). Etanercept treatment resulted in metabolic profiles that were shifted from both severe untreated ($Q^2 = 0.645$) and controls ($Q^2 = 0.534$), giving a unique pharmacological phenotype. However, the Etanercept vs control OPLS-DA model was the weakest of all generated models ($p = 2.76 \times 10^{-4}$), indicating that the treated cohort had a metabolic profile most similar to the controls. All model statistics are provided in Table S8.

Biochemical pathway enrichment analysis of the psoriasis-associated metabolic perturbations in common to both cohorts (Table 2) was used to identify significant perturbations ($p \leq 0.05$) in 10 major biochemical pathways (Table S9). Partial correlation networks were calculated to analyze empirical metabolite–metabolite relationships in the context of the identified psoriasis-associated metabolic perturbations (Figure 3). On the basis of the network topology, the three most psoriasis-impacted pathways were those of alanine, aspartate, and glutamate metabolism (hsa00250); glycine, serine, and threonine metabolism (hsa00260); and arginine and proline metabolism (hsa00330). In particular, there was a dominant psoriasis-dependent increase in the majority of urea cycle intermediates including aspartate, arginine, ornithine, and citrulline. The confirmed changes in metabolites (Table 2) are highlighted in these networks (thick borders) and can be classified into three major correlated clusters (Figure 3A): (1) cytidine, cystathionine, acetylglucosamine, hydroxyproline, and taurine; (2) ornithine, arginine, threonine, methionine, glutamine, glycine, citrulline, and proline; and (3) phenylalanine,

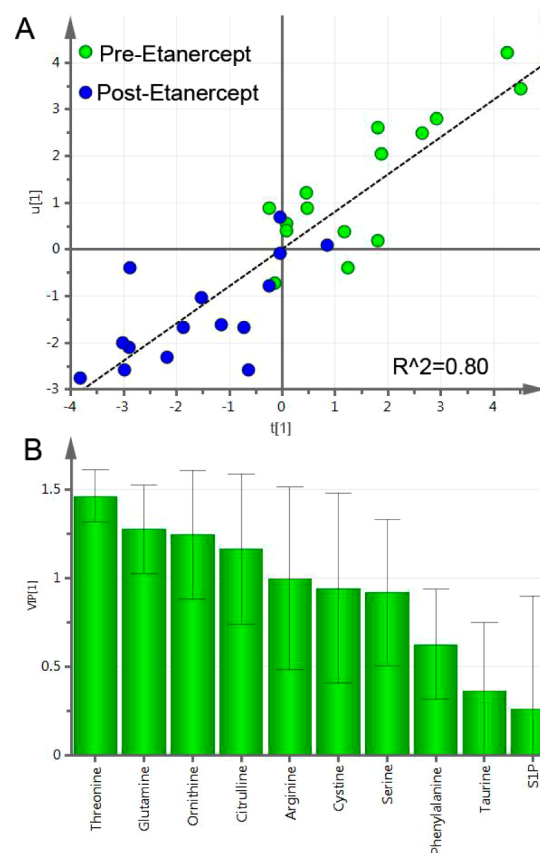


Figure 1. PLS inner relation between the 10 metabolites identified to correlate ($r \geq 0.5$) with the psoriasis area and severity index (PASI) in severe psoriasis patients pre- and post-treatment with Etanercept (Table 3). (A) The inner relation for severe psoriasis and treated severe psoriasis patients from the validation cohort ($R^2 = 0.80$). For untreated severe psoriasis only, $R^2 = 0.82$; for mild psoriasis only, $R^2 = 0.32$; and for mild, severe untreated, and treated psoriasis combined, $R^2 = 0.78$. For the exploratory cohort, $R^2 = 0.91$ for severe psoriasis, $R^2 = 0.49$ for mild and severe psoriasis combined, and $R^2 = 0.26$ for mild psoriasis only. (B) The variable importance in projection (VIP) plot displaying the relative contributions of the individual metabolites to the inner relation. SIP=sphingosine-1-phosphate.

cystine, GlcCer(C16:0), aspartate, and glutamate. Metabolic changes within these three clusters, with the exception of cystathionine, were positively correlated and increased with psoriasis severity (Table 3). Etanercept treatment of severe psoriasis patients predominantly impacted cluster 2 metabolites (Figure 3B). Comparison of the Etanercept treated group to healthy controls in the validation cohort (Figure 3C) revealed normalization in the majority of the previously identified psoriasis-associated metabolic perturbations with the exception of cystathionine and cystine.

DISCUSSION

There is an extensive body of literature on psoriasis; however, to date, there has been limited work investigating the underlying metabolic processes associated with the disease.³⁰ To the best of our knowledge, this is the first study utilizing nontargeted metabolomics to study the effect of psoriasis severity and the impact of Etanercept treatment on metabolism. Comparisons of plasma metabolic profiles of psoriasis patients suggest that the mild and severe disease states are not, from a metabolic perspective, distinct pathologies but a progression of

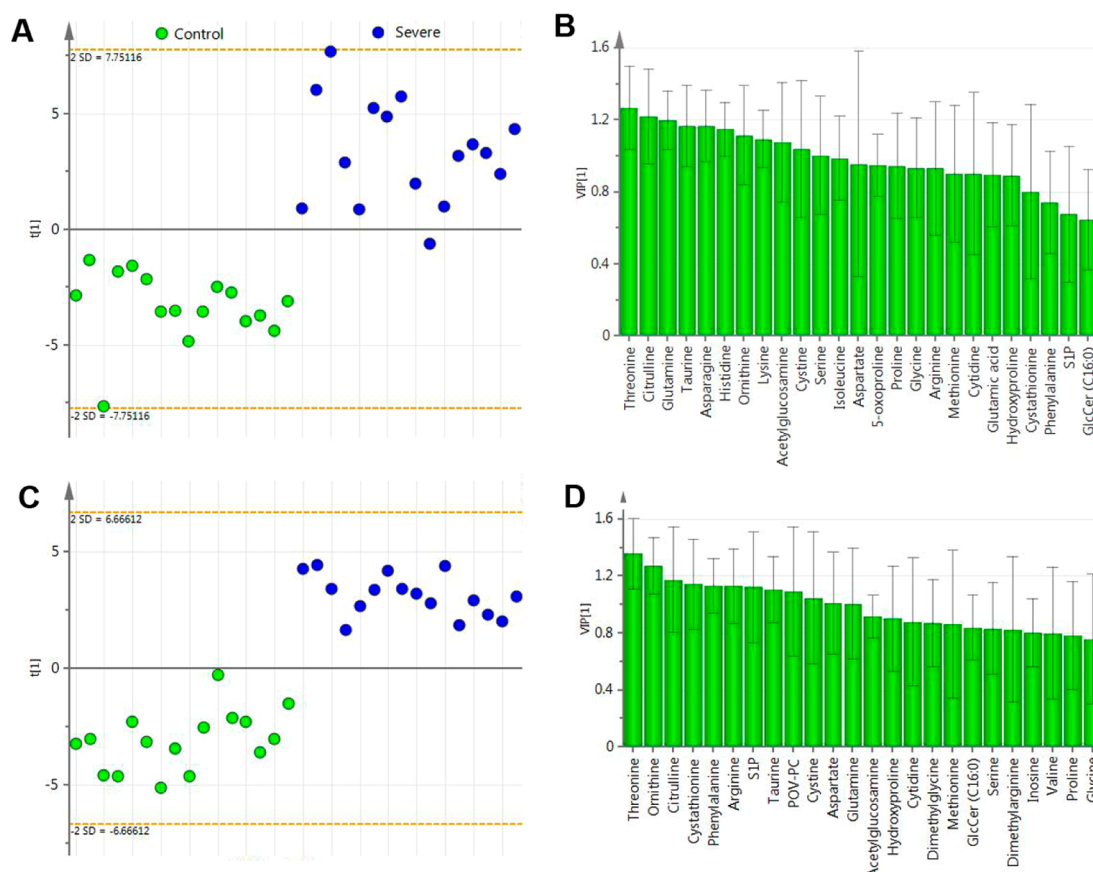


Figure 2. OPLS-DA scores and variable importance in projection (VIP) plots from the curated models following 2 rounds of variable selection as described in the Experimental Section. (A) Scores plot of control vs severe psoriasis in the exploratory cohort ($R^2Y = 0.762$ $Q^2 = 0.741$, CV ANOVA $p = 3.2 \times 10^{-9}$, 1 + 0 components); (B) VIP plot of control vs severe psoriasis in the exploratory cohort; (C) scores plot of control vs severe psoriasis in the validation cohort ($R^2Y = 0.895$ $Q^2 = 0.891$, CV ANOVA $p = 1.1 \times 10^{-14}$, 1 + 0 components); (D) VIP plot of control vs severe psoriasis in the validation cohort. S1P=sphingosine-1-phosphate.

the disease along a shared metabolic continuum. However, although distinct shifts in the circulatory metabolic profiles of severe psoriasis patients were observed, it is unclear as to the corresponding mechanism responsible.

Psoriasis severity was associated with an increase in three intermediates of the urea cycle (citrulline, ornithine, and arginine). Shifts in arginine and urea cycle metabolism have been previously reported in psoriatic skin lesions,³¹ and similar shifts in urea cycle intermediates,³² as well as changes in glutamine and glutamate, have been associated with wound healing.³³ The commonality in markers for psoriasis and wound healing is not surprising given that both psoriasis^{34,35} and wound healing^{36–38} involve the production of new keratinocytes. The urea cycle is an entry to the pathway for the synthesis of polyamines, which are essential hormones in cell proliferation, a hallmark of keratinocytosis in psoriasis.³⁹ The polyamine requirement may promote the mobilization of the urea cycle intermediate arginine from its sites of synthesis to the skin, resulting in the observed enhanced plasma levels.

Protein synthesis demand in the proliferating skin could also explain the elevated amino acid profile in plasma. Psoriasis is associated with changes in protein expression.⁴⁰ Cornification of the epidermis requires different scaffolding proteins than that in healthy cells, and a collection of support proteins such as small proline-rich proteins (SPRP), hornirine (HNRN), and late cornified envelope 3 A (LCE3A) were elevated up to 500 times in psoriasis skin compared to that in healthy skin.⁴⁰ The

production of these psoriasis-enriched proteins postulates an enhanced influx of amino acids. The requirements of this process agree largely with the observed increases in circulating amino acids. The most represented amino acids in the regulated proteins in psoriasis were serine, proline, glycine, and glutamine. This profile was not altered when a score of fold change (psoriasis vs healthy) of protein expression was calculated (Table S10). To add to the requirement burden, the major amino acids in human collagen 1 alpha are glycine (27%) and proline (18%). While collagen is produced in the dermis, which does not thicken in psoriasis, there are indications that collagen turnover is higher in psoriasis patients, with reported enhanced activity of collagen breakdown enzymes prolydase⁴¹ and matrix metalloproteinase MMP1⁴² (the latter being 13 times higher in psoriasis patients compared to that in healthy controls). Hydroxyproline, a marker for tissue collagen degradation,⁴³ was upregulated in severe psoriasis patients and normalized by Etanercept treatment. This agrees with Garvican et al., who showed the ability of IL-1 or TNF α to promote collagen degradation in ovine cartilage.⁴⁴ The modest correlation of hydroxyproline with PASI score may indicate different susceptibility of subjects, and further investigations are necessary to examine if this susceptibility is reflected with incidence of psoriatic arthritis.

Another potential explanation for the observed increase of circulating amino acids would be due to cachexia or wasting syndrome, which is the loss of lean body mass that can

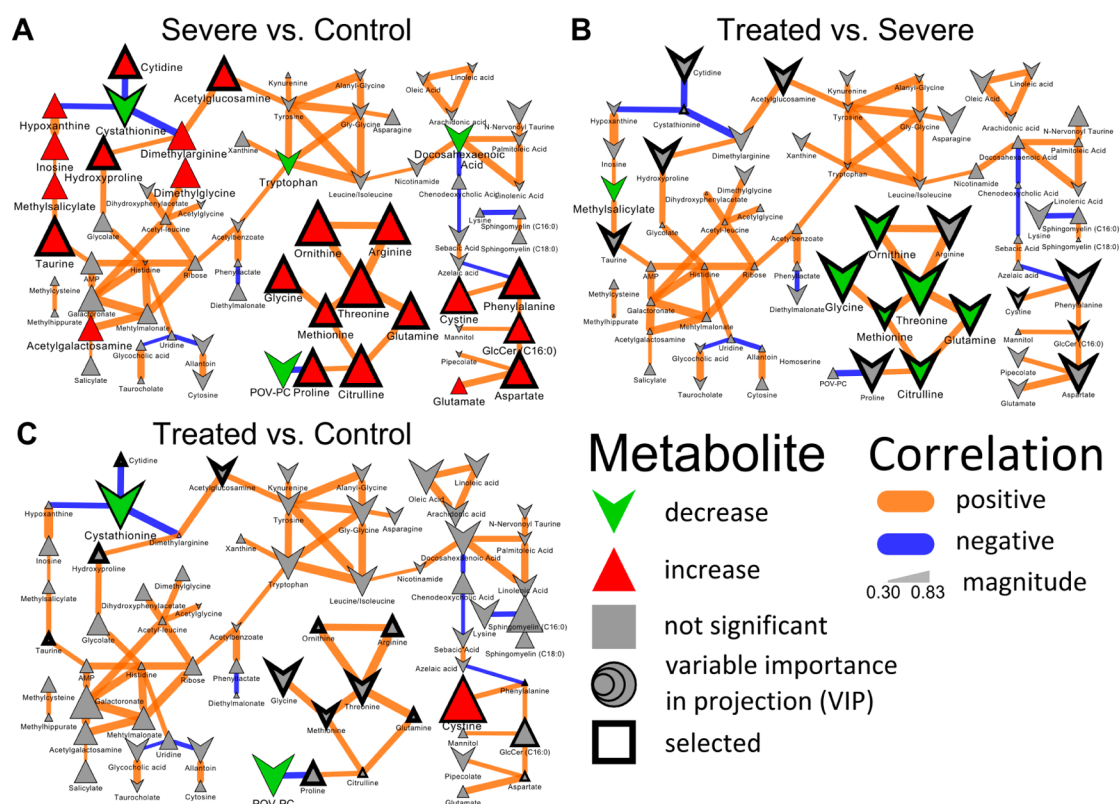


Figure 3. Dependency network displaying plasma metabolite relationships in psoriasis in the context of the noted metabolic perturbations between (A) severe untreated psoriasis and control, (B) severe treated and severe untreated psoriasis, and (C) severe treated psoriasis and control patients. Metabolites are connected based on partial correlation defined relationships, and edge color and width display the direction and magnitude of the FDR-adjusted Spearman rank order coefficient of correlation ($p_{adj} \leq 0.05$). Vertices represent metabolites, with the shape and color displaying relative direction and statistical significance ($p_{adj} \leq 0.05$) of the metabolic change for each respective comparison (i.e., panel A displays changes in severe psoriasis patients relative to controls). Metabolites are sized according to each comparison's respective OPLS-DA model VIP (Figure 2), and species in common in the exploratory and validation models' selected feature sets are highlighted with thick black borders.

accompany systemic inflammatory diseases.⁴⁵ Cachexia has been linked with psoriasis,⁴⁶ and cytokine inhibitors (e.g., anti-TNF α) have been suggested in the treatment of cachexia.⁴⁷ TNF α in particular is thought to play a role in both the anorexic effect via neuronal leptin receptors⁴⁸ as well as muscle wasting by enhancing protein ubiquitination.⁴⁹ A cachectic state of psoriasis patients has been suggested due to a dual role of TNF, evidenced by the increase in BMI during anti-TNF α treated patients.^{50,51} Accordingly, it is possible that increased muscle protein breakdown, a hallmark of cachexia, may explain the higher levels of circulating amino acids observed in subjects with severe psoriasis. Muscle wasting has been reported in other autoimmune diseases such as rheumatoid arthritis;⁵² however, this may not be associated with changes in body weight.⁵³ In our study, BMI was marginally higher in severe psoriasis patients (Table 1; $p = 0.07$), whereas the BMI values of each subject did not change following treatment ($p = 1.0$). Treatment with anti-TNF α has previously been reported to increase BMI,⁵⁴ but this was primarily due to increases in fat-free mass, which was not examined in the current cohort.

Cachexia has not been widely studied from a metabolic perspective, and there is no consensus on plasma levels of metabolites in cachectic patients or animal models. Peters et al. showed that in a tumor-bearing mouse model plasma amino acids were upregulated.⁵⁵ O'Connell et al. reported changes in lipids, glycerol, and glucose, but not amino acids, in the plasma of a murine cancer cachexia model.⁵⁶ A follow up study observed an increase in urea cycle amino acids and decreased

glycine, alanine, and serine in skeletal muscle.⁵⁷ Ubhi et al. observed a slightly significant ($p = 0.05$ – 0.1) increase in plasma amino acids of cachectic compared to noncachectic COPD patients.⁵⁸ Moreover, a number of cachectic studies exhibited lower levels of circulating amino acids during cachexia in clinical as well as animal studies.^{59–61} However, a down-regulation of circulating branched-chain amino acids, which is thought to be a hallmark of cachexia,⁶² was not observed in the current study. Accordingly, although it is unlikely that the observed shifts in circulating amino acids are due to cachexia, further evaluation is warranted.

The dominant effect of Etanercept treatment was observed in normalizing the plasma levels of a large cluster of positively correlated metabolites consisting of ornithine, arginine, proline, citrulline, glycine, glutamine, threonine, and methionine (Figure 3), specifically within the arginine/proline and glycine, serine, and threonine pathways (Table S9). The biochemical mechanism leading to the Etanercept-dependent reduction in these metabolites is unclear. However, blocking the immune (autoimmune) response can lead to a reduced signal for collagen and other keratinocyte-specific structural protein production as well as keratinocytosis, resulting in a diminished requirement for these metabolites. Etanercept acts by inhibiting the activity of the cytokine TNF α ,¹⁵ which is involved in a wide range of biological activities. TNF α can modulate the activity of nitric oxide synthase (NOS),⁶³ which is involved in the production of nitric oxide from the conversion of arginine to citrulline.⁶⁴ If Etanercept treatment, through inhibition of

TNF α , was impacting NOS activity, then shifts would be expected in the ratio of the citrulline-to-arginine concentration following treatment. However, a large reduction in all urea cycle metabolites, including arginine and citrulline, was observed, which does not support the modulation of NOS activity as a mode of action of treatment. Similarly, there are no reported mechanisms by which Etanercept may lead to reductions in intermediates of glycine, serine, and threonine metabolism. Etanercept could affect these metabolites through modulation of NOS, for example, by modulating the flux of aspartate between the urea cycle and threonine production. However, an analysis of metabolite partial correlations (Figure 3) reveals that aspartate levels are not directly linked to urea cycle intermediates but instead to glutamate. Of the 20 metabolites identified to shift with psoriasis, only cystathionine and cystine were not normalized to healthy levels following Etanercept treatment (Table 2 and Figure 3). Cystathionine was not correlated with PASI scores prior to treatment (Table 3), which may explain the lack of response and suggests a distinct mechanism. The fact that circulating amino acid levels returned to normal following anti-TNF α treatment in combination with the strong correlation to PASI score (before and after treatment) indicates that amino acid metabolism is a good marker for anti-TNF α responsiveness, as indicated by Kapoor et al.⁶⁵

Psoriasis patients are at increased risk of metabolic syndrome and diabetes,¹⁰ which share the common element of insulin resistance. The excess amino acid availability can stimulate the nutrient-sensitive mTOR/S6K pathway and inhibit serine phosphorylation of insulin receptor substrate 1, which can lead to an impairment in insulin-stimulated glucose disposal in skeletal muscles and insulin-mediated inhibition of glucose production.⁶⁶ Accordingly, although the chronic inflammatory status of psoriasis certainly plays a direct role in the development of insulin resistance, the observed enhanced circulating levels of amino acids suggest the hypothesis that the mTOR/S6K pathway may contribute to this risk. However, the validation of this tentative hypothesis warrants further investigation.

CONCLUSIONS

Although the severity of psoriasis is clearly linked to levels of circulating amino acids, the responsible mechanism(s) for the observed shifts are unclear. The observed increased levels may be due to keratinocyte hyperproliferation, increased proteolysis due to cachexia, or other unknown pathways. During hyperproliferation, the increased demand of protein building units, and specifically proline, may lead to a strong shift in amino acid profiles. Alternatively, it can be hypothesized that individuals with severe psoriasis are cachectic. There is a paucity of information on cachexia in psoriasis, but the majority of studies report an increase in BMI, which is not affected by Etanercept treatment in this study. Accordingly, further investigations are required to understand the significance of the observed amino acid shifts. It is clear that Etanercept treatment significantly shifts the metabolic profiles of psoriasis patients, reversing the distinct psoriasis metabolotype to that observed in healthy individuals, suggesting that focused metabolic profiling can be used to monitor patient response to therapeutic intervention systematically. The strong correlation of disease severity scoring with the metabolite levels indicates that the observed metabolic shift reflects a trajectory of disease progress rather than distinct disease pathologies. It is

also possible that circulating amino acid profiles could be used as markers of both disease severity as well as responsiveness to treatment.

ASSOCIATED CONTENT

Supporting Information

Materials and Methods: Detailed description of the methods used for analyzing the samples, data processing, safety considerations, and metabolite annotation. Table S1: Analytical internal standards used for HILIC and RP mode metabolomic analysis. Table S2: List of the chemical reference standards used for annotating metabolite features. Table S3: Summary of metabolic perturbations associated with psoriasis disease severity for the exploratory cohort. Table S4: Summary of metabolic perturbations associated with psoriasis disease severity for the validation cohort. Table S5: Changes in putatively identified (accurate mass) metabolite features in severe psoriasis relative to controls in the exploratory cohort. Table S6: Changes in putatively identified (accurate mass) metabolite features in severe psoriasis relative to controls in the validation cohort. Table S7: Changes in putatively identified (accurate mass) metabolite features in severe psoriasis relative to controls in the treatment cohort. Table S8: OPLS-DA model classification performance statistics for the exploratory and validation cohorts. Table S9: Biochemical pathway enrichment analysis of psoriasis-associated metabolic perturbations in common to the exploratory and validation cohorts. Table S10: Requirement of amino acids for the regulated proteins in psoriasis. This material is available free of charge via the Internet at <http://pubs.acs.org>.

AUTHOR INFORMATION

Corresponding Authors

*(M.S.) Phone: +46 08-517 733 48. E-mail: mona.stahle@ki.se.
*(C.E.W.) Phone: +46 08-524 876 30. Fax: +46 (0)8 736-0439. E-mail: craig.wheelock@ki.se.

Author Contributions

[†]M.A.K. and S.G.S. contributed equally to this work.

Notes

The authors declare no competing financial interest.

ACKNOWLEDGMENTS

We thank research nurse Helena Griehsel for excellent technical assistance. D.G. was supported by NIH Metabolomics Center grant no. DK097154. M.S. acknowledges support from the Swedish Research Council (K2012-57X-14202-11-6 and CERIC Linné Center), Stockholm County Council (20120059), Hudfonden, and Psoriasisfonden. C.E.W. was supported by the Center for Allergy Research (Cfa) and the Karolinska Institutet.

REFERENCES

- (1) Rachakonda, T. D.; Schupp, C. W.; Armstrong, A. W. Psoriasis prevalence among adults in the United States. *J. Am. Acad. Dermatol.* **2014**, *70*, 512–516.
- (2) Benoit, S.; et al. Elevated serum levels of calcium-binding S100 proteins A8 and A9 reflect disease activity and abnormal differentiation of keratinocytes in psoriasis. *Br. J. Dermatol.* **2006**, *155*, 62–66.
- (3) Henseler, T.; Christophers, E. Psoriasis of early and late onset: characterization of two types of psoriasis vulgaris. *J. Am. Acad. Dermatol.* **1985**, *13*, 450–456.

- (4) McGonagle, D.; Lories, R. J. U.; Tan, A. L.; Benjamin, M. The concept of a "synovio-entheseal complex" and its implications for understanding joint inflammation and damage in psoriatic arthritis and beyond. *Arthritis Rheum.* **2007**, *56*, 2482–2491.
- (5) Mease, P. J.; et al. Etanercept in the treatment of psoriatic arthritis and psoriasis: a randomised trial. *Lancet* **2000**, *356*, 385–390.
- (6) Genetic Analysis of Psoriasis Consortium & the Wellcome Trust Case Control Consortium. A genome-wide association study identifies new psoriasis susceptibility loci and an interaction between HLA-C and ERAP1. *Nat. Genet.* **2010**, *42*, 985–990.
- (7) Enerbäck, C.; Martinsson, T.; Inerot, A.; Wahlström, J.; Enlund, F.; Yhr, M.; Swanbeck, G. Evidence that HLA-Cw6 determines early onset of psoriasis, obtained using sequence-specific primers (PCR-SSP). *Acta Derm.-Venereol.* **1997**, *77*, 4.
- (8) Nestle, F. O.; Kaplan, D. H.; Barker, J. Psoriasis. *N. Engl. J. Med.* **2009**, *361*, 496–509.
- (9) Carrascosa, J. M.; et al. Obesity and psoriasis: inflammatory nature of obesity, relationship between psoriasis and obesity, and therapeutic implications. *Actas Dermo-Sifiliogr.* **2014**, *105*, 31–44.
- (10) Azfar, R. S.; et al. Increased risk of diabetes mellitus and likelihood of receiving diabetes mellitus treatment in patients with psoriasis. *Arch. Dermatol.* **2012**, *148*, 995–1000.
- (11) Ma, C.; Harskamp, C. T.; Armstrong, E. J.; Armstrong, A. W. The association between psoriasis and dyslipidaemia: a systematic review. *Br. J. Dermatol.* **2013**, *168*, 486–495.
- (12) Azfar, R. S.; Gelfand, J. M. Psoriasis and metabolic disease: epidemiology and pathophysiology. *Curr. Opin. Rheumatol.* **2008**, *20*, 416–422.
- (13) Schön, M. P.; Boehncke, W.-H. Psoriasis. *N. Engl. J. Med.* **2005**, *352*, 1899–1912.
- (14) Iyer, S.; Yamauchi, P.; Lowe, N. J. Etanercept for severe psoriasis and psoriatic arthritis: observations on combination therapy. *Br. J. Dermatol.* **2002**, *146*, 118–121.
- (15) Sprott, H.; Glatzel, M.; Michel, B. A. Treatment of myositis with etanercept (Enbrel®), a recombinant human soluble fusion protein of TNF- α type II receptor and IgG1. *Rheumatology* **2004**, *43*, 524–526.
- (16) Lynch, M.; Kirby, B.; Warren, R. B. Treating moderate to severe psoriasis—best use of biologics. *Expert Rev. Clin. Immunol.* **2014**, *10*, 269–279.
- (17) Onesti, J. K.; Guttridge, D. C. Inflammation based regulation of cancer cachexia. *BioMed Res. Int.* **2014**, *2014*, 7.
- (18) Petersen, A.-K.; et al. Epigenetics meets metabolomics: an epigenome-wide association study with blood serum metabolic traits. *Hum. Mol. Genet.* **2014**, *23*, 534–545.
- (19) Suhre, K.; Gieger, C. Genetic variation in metabolic phenotypes: study designs and applications. *Nat. Rev. Genet.* **2012**, *13*, 759–769.
- (20) Fredriksson, T.; Pettersson, U. Severe psoriasis—oral therapy with a new retinoid. *Dermatologica* **1978**, *157*, 238–244.
- (21) Chambers, M. C.; et al. A cross-platform toolkit for mass spectrometry and proteomics. *Nat. Biotechnol.* **2012**, *30*, 918–920.
- (22) Smith, C. A.; Want, E. J.; O'Maille, G.; Abagyan, R.; Siuzdak, G. XCMS: processing mass spectrometry data for metabolite profiling using nonlinear peak alignment, matching, and identification. *Anal. Chem.* **2006**, *78*, 779–787.
- (23) R Development Core Team R: *A language and environment for statistical computing*; R Foundation for Statistical Computing; Vienna, Austria, 2011; <http://www.R-project.org/>.
- (24) Benjamini, Y.; Hochberg, Y. Controlling the false discovery rate—a practical and powerful approach to multiple testing. *J. R. Stat. Soc. B* **1995**, *57*, 289–300.
- (25) Dabney, A.; Storey, J. D. *qvalue: Q-value estimation for false discovery rate control*, 2013; <http://www.bioconductor.org/packages/release/bioc/html/qvalue.html>.
- (26) Wheelock, A. M.; Wheelock, C. E. Trials and tribulations of 'omics data analysis: assessing quality of SIMCA-based multivariate models using examples from pulmonary medicine. *Mol. Biosyst.* **2013**, *9*, 2589–2596.
- (27) Xia, J.; Mandal, R.; Sinelnikov, I. V.; Broadhurst, D.; Wishart, D. S. MetaboAnalyst 2.0—a comprehensive server for metabolomic data analysis. *Nucleic Acids Res.* **2012**, *40*, W127–W133.
- (28) Castelo, R.; Roverato, A. Reverse engineering molecular regulatory networks from microarray data with qp-graphs. *J. Comput. Biol.* **2009**, *16*, 213–227.
- (29) Shannon, P.; et al. Cytoscape: a software environment for integrated models of biomolecular interaction networks. *Genome Res.* **2003**, *13*, 2498–2504.
- (30) Lu, C.; Deng, J.; Li, L.; Wang, D.; Li, G. Application of metabolomics on diagnosis and treatment of patients with psoriasis in traditional Chinese medicine. *Biochim. Biophys. Acta* **2014**, *1844*, 280–288.
- (31) Abeyakirithi, S.; et al. Arginase is overactive in psoriatic skin. *Br. J. Dermatol.* **2010**, *163*, 193–196.
- (32) Albina, J. E.; Mills, C. D.; Henry, W. L.; Caldwell, M. D. Temporal expression of different pathways of L-arginine metabolism in healing wounds. *J. Immunol.* **1990**, *144*, 3877–3880.
- (33) Albina, J. E.; Abate, J. A.; Mastrofrancesco, B. Role of ornithine as a proline precursor in healing wounds. *J. Surg. Res.* **1993**, *55*, 97–102.
- (34) Prinz, J. C.; et al. T cell clones from psoriasis skin lesions can promote keratinocyte proliferation in vitro via secreted products. *Eur. J. Immunol.* **1994**, *24*, 593–598.
- (35) Schön, M. P.; Ruzicka, T. Psoriasis: the plot thickens. *Nat. Immunol.* **2001**, *2*, 91.
- (36) Martin, P. Wound healing—aiming for perfect skin regeneration. *Science* **1997**, *276*, 75–81.
- (37) Baker, E. A.; Leaper, D. J. Proteinases, their inhibitors, and cytokine profiles in acute wound fluid. *Wound Repair Regen.* **2000**, *8*, 392–398.
- (38) Mann, A.; Breuhahn, K.; Schirmacher, P.; Blessing, M. Keratinocyte-derived granulocyte-macrophage colony stimulating factor accelerates wound healing: stimulation of keratinocyte proliferation, granulation tissue formation, and vascularization. *J. Invest. Dermatol.* **2001**, *117*, 1382–1390.
- (39) Wei, L. H.; Wu, G.; Morris, S. M.; Ignarro, L. J. Elevated arginase I expression in rat aortic smooth muscle cells increases cell proliferation. *Proc. Natl. Acad. Sci. U.S.A.* **2001**, *98*, 9260–9264.
- (40) de Koning, H. D.; et al. Expression profile of cornified envelope structural proteins and keratinocyte differentiation-regulating proteins during skin barrier repair. *Br. J. Dermatol.* **2012**, *166*, 1245–1254.
- (41) Guven, B.; Can, M.; Genc, M.; Koca, R. Serum prolidase activity in psoriasis patients. *Arch. Dermatol. Res.* **2013**, *305*, 473–476.
- (42) Starodubtseva, N. L.; Sobolev, V. V.; Soboleva, A. G.; Nikolaev, A. A.; Bruskin, S. A. [Expression of genes for metalloproteinases (MMP-1, MMP-2, MMP-9, and MMP-12) associated with psoriasis]. *Genetika* **2011**, *47*, 1254–1261.
- (43) Kindt, E.; Gueneva-Boucheva, K.; Rekhter, M. D.; Humphries, J.; Hallak, H. Determination of hydroxyproline in plasma and tissue using electrospray mass spectrometry. *J. Pharm. Biomed. Anal.* **2003**, *33*, 1081–1092.
- (44) Garvican, E. R.; Vaughan-Thomas, A.; Redmond, C.; Gabriel, N.; Clegg, P. D. MMP-mediated collagen breakdown induced by activated protein C in equine cartilage is reduced by corticosteroids. *J. Orthop. Res.* **2010**, *28*, 370–378.
- (45) Schiaffino, S.; Dyar, K. A.; Ciciliot, S.; Blaauw, B.; Sandri, M. Mechanisms regulating skeletal muscle growth and atrophy. *FEBS J.* **2013**, *280*, 4294–4314.
- (46) Yamanaka, K.; et al. Persistent release of IL-1s from skin is associated with systemic cardio-vascular disease, emaciation and systemic amyloidosis: the potential of anti-IL-1 therapy for systemic inflammatory diseases. *PLoS One* **2014**, *9*, e104479.
- (47) Straub, R. H.; Cutolo, M.; Buttgerit, F.; Pongratz, G. Energy regulation and neuroendocrine-immune control in chronic inflammatory diseases. *J. Int. Med.* **2010**, *267*, 543–560.
- (48) Gan, L.; et al. TNF- α up-regulates protein level and cell surface expression of the leptin receptor by stimulating its export via a PKC-dependent mechanism. *Endocrinology* **2012**, *153*, 5821–5833.

- (49) LI, Y.-P.; et al. TNF- α increases ubiquitin-conjugating activity in skeletal muscle by up-regulating UbcH2/E220k. *FASEB J.* **2003**, *17*, 1048–1057.
- (50) Florin, V.; Cottencin, A. C.; Delaporte, E.; Staumont-Sallé, D. Body weight increment in patients treated with infliximab for plaque psoriasis. *J. Eur. Acad. Dermatol. Venereol.* **2013**, *27*, e186–e190.
- (51) Saraceno, R.; et al. Effect of anti-tumor necrosis factor- α therapies on body mass index in patients with psoriasis. *Pharmacol. Res.* **2008**, *57*, 290–295.
- (52) Summers, G. D.; Metsios, G. S.; Stavropoulos-Kalinoglou, A.; Kitas, G. D. Rheumatoid cachexia and cardiovascular disease. *Nat. Rev. Rheumatol.* **2010**, *6*, 445–451.
- (53) Llovera, M.; López-Soriano, F. J.; Argilés, J. M. Effects of tumor necrosis factor- α on muscle-protein turnover in female Wistar rats. *J. Natl. Cancer Inst.* **1993**, *85*, 1334–1339.
- (54) Renzo, L. D.; et al. Prospective assessment of body weight and body composition changes in patients with psoriasis receiving anti-TNF- α treatment. *Dermatol. Ther.* **2011**, *24*, 446–451.
- (55) Peters, S.; van Helvoort, A.; Kegler, D.; Argilés, J.; Luiking, Y.; Laviano, A.; van Bergenhenegouwen, J.; Deutz, N.; Haagsman, H.; Gorselink, M.; van Norren, K. Dose-dependent effects of leucine supplementation on preservation of muscle mass in cancer cachectic mice. *Oncol. Rep.* **2011**, *26*, 247–254.
- (56) O'Connell, T.; et al. Metabolomic analysis of cancer cachexia reveals distinct lipid and glucose alterations. *Metabolomics* **2008**, *4*, 216–225.
- (57) Der-Torossian, H.; et al. Metabolic derangements in the gastrocnemius and the effect of Compound A therapy in a murine model of cancer cachexia. *J. Cachexia Sarcopenia Muscle* **2013**, *4*, 145–155.
- (58) Ubhi, B. K.; et al. Targeted metabolomics identifies perturbations in amino acid metabolism that sub-classify patients with COPD. *Mol. BioSyst.* **2012**, *8*, 3125–3133.
- (59) Pearlstone, D. B.; et al. Effect of enteral and parenteral nutrition on amino acid levels in cancer patients. *JPEN, J. Parenter. Enteral Nutr.* **1995**, *19*, 204–208.
- (60) Blumberg, D.; Hochwald, S.; Burt, M.; Donner, D.; Brennan, M. F. Tumor necrosis factor alpha stimulates gluconeogenesis from alanine in vivo. *J. Surg. Oncol.* **1995**, *59*, 220–225.
- (61) Preston, T.; et al. Fibrinogen synthesis is elevated in fasting cancer patients with an acute phase response. *J. Nutr.* **1998**, *128*, 1355–1360.
- (62) Ubhi, B. K.; et al. Metabolic profiling detects biomarkers of protein degradation in COPD patients. *Eur. Respir. J.* **2012**, *40*, 345–355.
- (63) Gazzinelli, R. T.; Eltoun, I.; Wynn, T. A.; Sher, A. Acute cerebral toxoplasmosis is induced by in vivo neutralization of TNF- α and correlates with the down-regulated expression of inducible nitric oxide synthase and other markers of macrophage activation. *J. Immunol.* **1993**, *151*, 3672–3681.
- (64) Castillo, L.; et al. Plasma arginine and citrulline kinetics in adults given adequate and arginine-free diets. *Proc. Natl. Acad. Sci. U.S.A.* **1993**, *90*, 7749–7753.
- (65) Kapoor, S. R.; et al. Metabolic profiling predicts response to anti-tumor necrosis factor α therapy in patients with rheumatoid arthritis. *Arthritis Rheum.* **2013**, *65*, 1448–1456.
- (66) Tremblay, F.; et al. Overactivation of S6 kinase 1 as a cause of human insulin resistance during increased amino acid availability. *Diabetes* **2005**, *54*, 2674–2684.